

DUMAND Note 80-25

**MONTE CARLO STUDIES OF DUMAND ARRAY PERFORMANCE****II. FURTHER WORK ON DETECTION OF MUON NEUTRINOS  
VIA SINGLE RECOIL MUONS.**

by  
 A. Roberts and V. J. Stenger  
 Hawaii DUMAND Center  
 Dept. of Physics and Astronomy, Univ of Hawaii, Honolulu, HI.

**ABSTRACT.** — Two arrays proposed at the 1980 DUMAND Summer Workshop/Symposium, namely a "MINI" array with 10m spacing, 100m overall dimension, and a "MIDI" array with 50m spacing, 500m overall dimension, have been evaluated by means of Monte Carlo studies, for their ability to detect and determine the direction of single muons. Other properties, such as cascade detection or multiple muon detection, have not been considered. The studies indicate that the 10m spacing is uneconomically small; the MINI array should have at least 15m, perhaps 20m spacing. The MIDI array, evaluated on the assumption of the availability of a Sea Urchin or other sensor with a sensitivity  $S = 6$ , can have a 50 - 55m spacing if the water transparency (attenuation length for Cerenkov light) is 25m, somewhat less if only 20m. The use of timing information materially improves angular resolution. The MINI array resolution should be 8 - 10mr, the MIDI 5mr. Higher sensitivity than  $S = 6$  is not particularly useful, nor are very large array spacings. With larger arrays (more sensor planes), considerable higher angular accuracy is possible, up to 1.5 mr.

**1. Introduction.**

The primary mode of use of DUMAND in neutrino astronomy appears to be the detection of muon neutrinos by means of the muons they produce in charged-current interactions. The direction of the muon is quite close to that of the neutrino, and thus it is desirable for the array to be able to measure muon direction to the limit set by the difference between muon and neutrino directions.

The background for the signal from extraterrestrial neutrinos is set by the neutrino flux produced in the atmosphere by cosmic rays. Although the primary flux is isotropic, the neutrino flux is not, except at very low and very high energies. It is, however, diffuse, and consequently, the signal-to-noise ratio for a point extraterrestrial source will be inversely proportional to the square of the angular error of the detector. Thus good angular resolution for muon tracks is the major design criterion for this purpose. For an extended discussion of the effect of angular resolution on extraterrestrial signal detection, see Ref. [5].

If the angular resolution is 10mr, the fraction of the average background within that angle is  $8.0 \times 10^{-6}$ ; at 5mr it is one-fourth as much. Since the

maximum expected atmospheric neutrino rates for a 1-km<sup>3</sup> detector are less than ~10<sup>5</sup>/year, the backgrounds will be less than one event/yr. Thus, the limit on detecting extraterrestrial neutrinos will not be the atmospheric background, but the strength of the observed signal, provided the angular resolutions discussed can be obtained.

In this report we present the results of comparative Monte Carlo studies performed since the Summer symposium, representing an attempt to answer some of the questions raised there and discussed in other papers in these proceedings. Many of the results of this work have been obtained, in less detail, in previous work by one of us (VJS) (3-4, also these proceedings).

## 2. Variables of the Problem.

The variables that define the properties of a DUMAND array event fall into two classes: properties of the array and external properties. The latter include the optical attenuation length of the water and the energy and direction of the incident muon. The array parameters may be enumerated as follows:

1. Array size, configuration, and spacing
2. Module sensitivity and threshold triggering levels
3. PMT (or sensor) time resolution

The event parameters include:

1. The number and position of the sensors triggered
2. The number of photoelectrons produced at each sensor
3. The time of arrival of the signal.

The track reconstruction has two components:

1. Space Fit: using only data on location of sensors triggered and the size of the signal in each.
2. Time Fit: Uses in addition to space data the observed time of arrival of the signal.

The task is to explore the multi-dimensional space defined by all these variables. The available tool is the Monte Carlo program DMC developed over the last two years, first by A. Roberts at Fermilab (1), and then much more extensively by Stenger and Taylor (2), and by Stenger (3,4) at Hawaii. Originally the program merely simulated muon tracks in sea-water, in order to investigate the possibility of measuring muon energies in DUMAND. Stenger and Taylor added an array-simulating program and the technique for passing arbitrary muons through the array, calculating the energy losses and their concomitant optical signals in the array sensors. This defined the array's response. Next, bubble chamber techniques for track reconstruction were adapted to the reconstruction of the muon tracks. Comparison of the "measured" and "true" tracks then yields a measure of the accuracy of track reconstruction.

Fits to the reconstructed track have been made by two procedures. One uses only the number and position of triggered sensors and the magnitude of the sensor response; this is the "space" fit. A second uses in addition the information on the time of arrival of the signal at each sensor, to which a gaussian error described by its standard deviation (TRES) is added at random. With this information, improved fits can be obtained, as we shall see. This is the "time" fit.

The exploration of the multi-dimensional space is necessarily an extensive one; with 10 dimensions and only 4 values for each, we need  $4^{10}$  or  $10^6$  points for a complete exploration. Fortunately, many parameters do not need to be explored in that detail; and the problem can be narrowed down to a readily manageable size.

### 3. Initial Array Parameters.

#### 3.1 Use of Cubic Arrays.

The arrays proposed at the 1980 DUMAND Workshop/Symposium served as the initial material for this study. For simplicity, both are taken as cubic; hexagonal arrays with the same volume and base surface area have approximately a 10% smaller DMAX than a cubic array, where DMAX is the largest distance from a point inside the array to the nearest sensor. In a cubic array with 10m spacing, DMAX is 8.66m; in a hexagonal array with spacing 10.75m (to get the same base area), DMAX is 7.96m. This is equivalent to an increase in the transparency of the water of about 10%, an effect that may be appraised by looking at the curves showing the effect of varying the attenuation length (Figs. 6, 8).

#### 3.2 Definition of Initial Arrays.

The two cubic arrays that served as a starting point, as defined by the 1980 Workshop (6), were:

1. A cube 100m on a side, with 10m spacing. This gives 11 sensors per side, or 1331 total; and a cross-sectional area of  $10^4 \text{ m}^2$  or  $0.01 \text{ km}^2$ , and a volume of  $10^6 \text{ m}^3$  or  $10^{-3} \text{ km}^3$ . This array is called the MINI-DUMAND, or MINI.
2. A cube scaled up from MINI by a factor of five: 500m on a side, with 50m spacing, 1331 sensors, a base area of  $0.25 \text{ km}^2$ , and a volume of  $0.125 \text{ km}^3$ . This array is called MIDI.

In addition, many other arrays were examined, to test the importance of sensor spacing and sensor sensitivity. The sensitivity of available or expected sensors is shown in the following table, which is taken from DUMAND Note 80-18 (7).

Table 3.1 Sensor Sensitivity.

SENSOR	PHOTOCATHODE AREA, $m^2$	SENSITIVITY, Stengers (No. of photoelectrons at $100g/m^2$ , at 20% photocathode efficiency)
<b>a) Direct-View</b>		
8" PMT	.0314	0.63
13" PMT	.080	1.61
Cylindrical, 0.4x1.0m	0.4	8.0
<b>b) WLS sensors</b>		
Sea Urchin*	0.3 equiv.	6.0

\*See Refs (8-10)

Since 8" tubes have been produced in some quantity, and the 13" tube is now undergoing evaluation of samples prior to going into production, it seems reasonable to regard these as available.

For MINI, the 13"-tube seems an obvious choice. Since the sensitivity of a hemispherical-cathode PMT is not isotropic, dropping to half at right angles to the axis, we assumed a sensitivity of 1.0 stenger to be on the safe side.

In contrast, a wide-spaced array like MIDI needs a more sensitive detector. The only available one at present is Sea Urchin, with a sensitivity of 6 stengers. This was accordingly adopted. The proposed cylindrical direct-view PMT is still on the drawing board (11).

### 3.3 Track Variation.

All the foregoing data were taken with single muon tracks; we have not yet investigated in more detail than previous studies (4) the performance with multiple tracks. With the exception of one short run in which the direction was varied, all the data were taken with a single geometrical path through the array, one that was nearly diagonal. The initial pseudo-random number (seed) was always the same, so that when an array parameter was altered, the comparison was always made with a set of identical tracks. Since the track-generating routine uses pseudo-random numbers to generate interactions along the tracks, successive tracks are different from each other, but two runs starting from the same pseudo-random seed will be identical.

A short run in which the muon direction was varied showed no large variations beyond those expected by chance, and the change of track length.

### 4. Time Fit.

The results of a run in which the time resolution TRES is varied are shown in Fig. 1. TRES is the standard deviation of a gaussian, and is thus about one-third the full time spread. The largest value in Fig. 1, TRES = 15nsec, corresponds to a rise time of about 40nsec, and gives little or no im-

provement over the space fit. Below that value the improvement is marked, the final angular error being proportional to TRES. The 4-nsec value adopted for most further work corresponds to the observed time spread for venetian-blind dynode photomultipliers, the sort we expect to use, and is thus realistic. In Fig. 1, the change of slope between MINI2 and MIDI arrays is marked; the wider spaced arrays appear to be inherently more accurate.

This observation is of great significance in considering the use of Sea Urchin. We estimate a worst case overall time spread of 22 ns in the light reaching the central PMT from a plane wave incident on Sea Urchin at right angles to the axis. This corresponds to a TRES of ca. 7ns; adding this in quadrature to the 4ns time resolution of the PMT, we obtain an effective TRES = 8ns for Sea Urchin, worst case. From Fig. 1, we see that this gives a factor of 2 loss in angular resolution. For the case of light incident axially (the direction of maximum sensitivity), the worst case light spread is 11 ns, giving an effective TRES of 6ns.

### 5. Initial Performance Data.

The first runs were taken with reasonable values for the several parameters, and the event parameters - particularly the muon energy - varied. The time fit parameter, TRES, was set at 4ns for nearly all runs, unless otherwise noted.

#### 5.1. MINI Performance: Introduction of MINI2.

For reasonable values of the parameters, the MINI array is clearly over-sensitive. Even minimum-ionizing tracks were found to trigger >50 sensors when the threshold was set at 2 photoelectrons. As we will see below, only 10 - 12 sensors are needed to give a good track fit in arrays of this size, so that this represents a considerable waste. Since an array for muon detection should be no denser than required for a good track fit, we increased the sensor spacing to 15 meters.

The resulting array, 150m on a side, was named MINI2, and took the place of MINI in subsequent work. Its performance, if anything, was superior to that of MINI; it worked well over a wider range of energies, from 50 GeV to at least 10 TeV. Both were satisfactory down to at least 50 GeV; below that the muon range is too short. Data on MINI and MINI2 performance at various energies are given in Figs. 2 and 3. The enormous improvement consequent upon the use of timing information is immediately apparent. The transparency for Figs. 2 - 7 is 25m.

#### 5.2. MIDI, and wider spacings.

Initial results on the MIDI array are shown in Fig. 4. The number of points on a MIDI track is considerably less than for a MINI2 track; but if anything, the fits are better, and the energy range wide; MIDI is good up to 100 TeV. Results with 75m and 100m spacing are shown in Figs. 5 and 6. At 75m the number of points on the track is insufficient to obtain a good fit below 100 TeV, and at 100m spacing a good fit is never obtained.

Fig. 7 shows the number of points on a track as a function of energy,

for different spacings. In most cases, the number increases above a few TeV, as the rate of energy loss of the muon increases. At 100m spacing the only signals seen are those due to bursts, and the track fit is never acceptable.

### **6. Water Transparency.**

The variation in the number of points on the track with water transparency for a fixed spacing is shown in Fig. 8. The effect is significant; but the change of spacing for the array to compensate for the change of transparency is not linear, provided we take the time fit as the criterion. The effect must be examined in detail for each case. If the spacing is marginal at 25m transparency, it may be excessive at 20m. This effect is illustrated in Fig. 9, which shows the angular resolution (time fit) as a function of transparency for several different spacings. For 30m spacing, there is merely a gradual improvement of time fit; at 65m a large effect is observed, since the number of points on the track drops below a critical value. The histograms of Fig. 10 illustrate the effect.

### **7. Variation of Array Spacing with Fixed Sensitivity.**

Figs. 11 and 12 show, for  $S = 6$  and  $S = 1$ , respectively, the variation with spacing of the number of points NPT and the angular resolution, for two different values of water attenuation. Dotted lines are added to guide the eye. It is notable that as the spacing increases, the angular resolution remains nearly constant until a critical value is reached (which we have called the "knee" of the curve), at which it deteriorates sharply. There is an appreciable difference between the locations of the knee at 20m and 25m transparencies; the knee moves from about 40m at 20m transparency, to 55m at 25m transparency. The break does not occur at the same value of NPT, but they are not markedly different.

Fig. 12, showing the data for  $S = 1$ , seems to indicate not quite so large a difference; the knees at 20m and 25m transparency occur at 22.5 and 25m respectively.

### **8. Variation of Sensor Sensitivity.**

The effects of varying the sensor sensitivity are of great importance, since they markedly affect the cost of the sensor and its complexity.

At 100m spacing the number of photoelectrons per hit is significantly higher than at smaller spacings. This means that in general the muon track itself is invisible, and signals are recorded only when a burst occurs on the track. Increasing sensitivity doesn't help much; the optical attenuation is overriding. Fig. 13 shows the performance data.

Fig. 14 shows the number of points per track as a function of sensitivity for spacings of 50 to 100m. The straight lines do not extrapolate to zero at zero sensitivity. At 100m no good fit is obtained even at  $S = 20$ , which appears to rule out the array suggested by Cline (12).

Fig. 15 shows how the time fit varies with sensitivity as the water

transparency or array size is changed. Note that a good operating point - the "knee" of the curve - is readily found for each case.

Fig. 16 shows a set of histograms of the time fit for 15m spacing, as the sensitivity is changed; fig. 17 does the same for the space fit.

#### 9. Effect of Increasing Array Dimensions.

Figs. 18 and 19 show the improvement in angular accuracy that can be achieved by doubling the dimensions of the array. Such an array, with eight times as many sensors, is of course far more expensive; but it shows that a sufficiently large DUMAND array is probably capable of measuring the direction of the recoil muon with all the precision warranted by the fact that the muon is not exactly in the same direction as the incident neutrino, even at very high energies.

#### 10. Graded Arrays.

A graded array, as suggested at the 1980 Workshop, combines both MINI and MIDI into a single array with high density at the center, less at the outside. We have not evaluated such arrays as yet; the present programs will require some modification to do so.

#### 11. Summary.

1. The 10 - 12 ns rise-time of venetian-blind PMT's will yield highly satisfactory angular resolutions: 8-10 mr for MINI, 5mr for MIDI.
2. MINI Array: the minimum desirable array spacing is 15m. At 15m spacing, the energy range of the array is 50 GeV - 10 TeV or more, and the angular accuracy 8-10mr for 25m water.
3. MIDI Array: With 50m spacing, S = 6, 25m water, the energy range is 300 GeV (limited by muon range) to 100 TeV. The accuracy is 5 mr if the time resolution is TRES = 4ns, the value appropriate to venetian-blind tubes. With Sea Urchin, values of TRES range from 5.5 to 8 ns in the worst cases; and thus the attainable resolution is probably 7-8 mr.
4. All array parameters must be tailored to the water transparency. Thus knowledge of the long-term stability of both water transparency and sensor sensitivity is essential.
5. Increase of sensitivity beyond S = 6 is not particularly useful.
6. S = 1 is perfectly adequate for MINI arrays. Accuracy increases slightly with increasing S.
7. Very large spacings (>75m for 25m water) are no good at any S.
8. With very large arrays (twice as many detector planes, or 8x as many sensors,) angular accuracies as high as 1.5 mr can be achieved.

REFERENCES

1. A. Roberts, "A Monte Carlo Study of the Measurement of Energy of Muons and Cascades in a DUMAND Optical Array," Vol. 1, p.275, Proc. 1978 DUMAND Summer Workshop, LaJolla, CA., A. Roberts, ed. DUMAND, Scripps Institution, LaJolla, 1979.
2. V. J Stenger, G. N. Taylor, and A. Roberts, Proc. 16th Intl. Cosmic Ray Conference, Kyoto, 1979, Vol. 10, p.373.
3. V. J. Stenger, "Computer Simulation of the DUMAND Optical Array," p.22, Proc. DUMAND Summer Workshop at Khabarovsk/Lake Baikal, USSR, 1979, J. Learned ed. Hawaii DUMAND Center, Honolulu, HI, 1980.
4. V. J. Stenger, "Latest Results on Monte Carlo Evaluation of the DUMAND Array," p. 187, Proc. 1980 DUMAND Signal Processing Workshop, Honolulu, HI., A. Roberts, ed. Hawaii DUMAND Center, Honolulu, 1980
5. V. J. Stenger, "Monte Carlo Studies of DUMAND Array Performance, I. Symposium Report", these proceedings.
6. Committee on Arrays, "Interim Report on Array Design,", these proceedings.
7. A. Roberts, "Recent Evolution of the DUMAND Array, and Consequences for Sensor Design," DUMAND Note 80-18; these proceedings.
8. D. McGibney, A. Roberts and U. Camerini, "The Sea Urchin Module. I. Survey of Design Problems." DUMAND Note 80-13; these proceedings.
9. D. McGibney and A. Roberts, "Design of the Sea Urchin Module. II. Spine Design." DUMAND Note 80-14; these proceedings.
10. A. Roberts and D. McGibney, "Design of the Sea Urchin Module. III. Experimental Measurements of Spine Efficiency and Redesign for Improved Sensitivity," DUMAND Note 80-23; these proceedings.
11. A. W. Wright, "Case for Very Large Photomultipliers - DUMAND", these proceedings.
12. D. B. Cline, "Neutrino Physics Possibilities with a Graded Sensor Array in DUMAND", these proceedings.

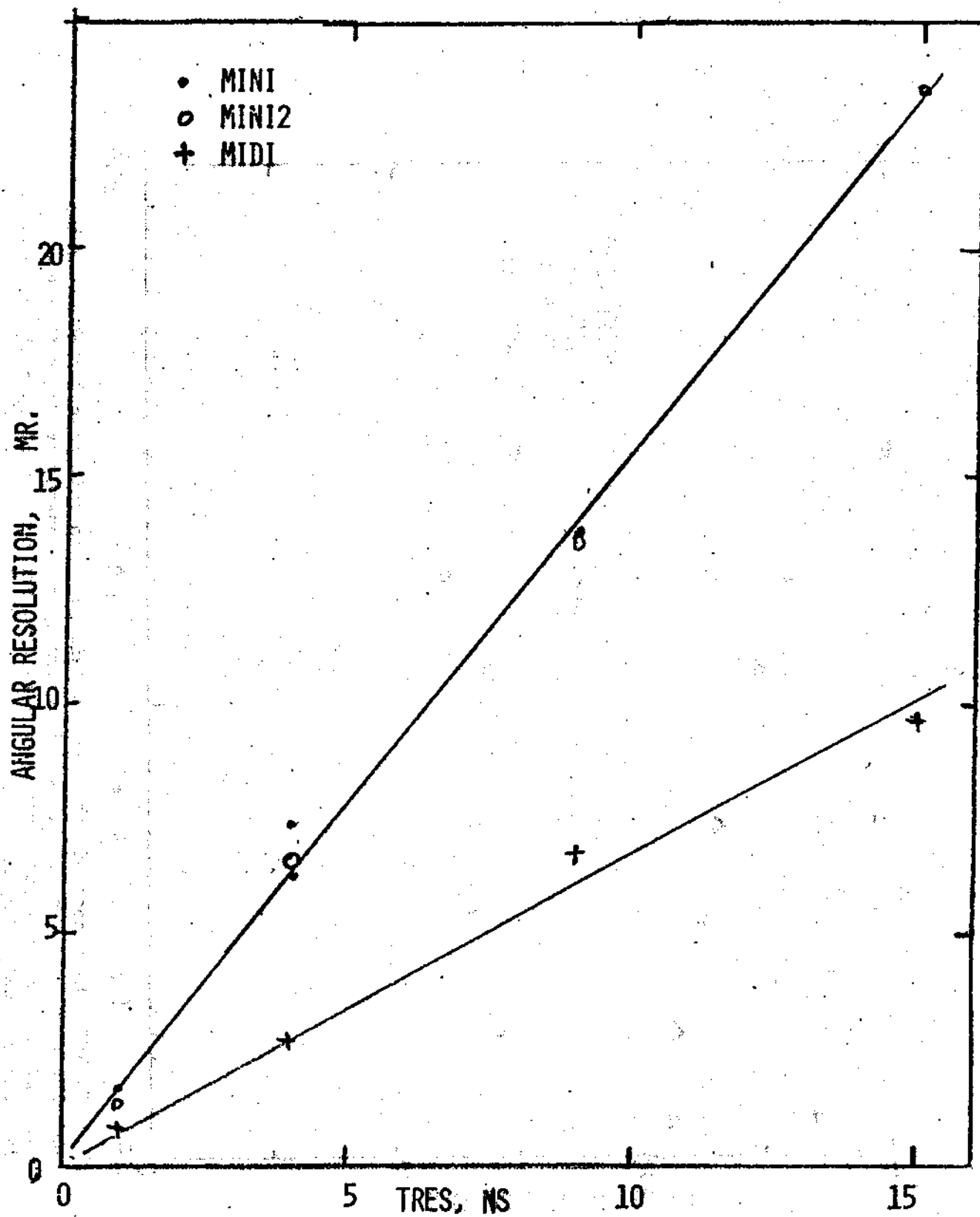


Fig. 1. Effect on the angular resolution of varying the time resolution TRES, the standard deviation of a gaussian time spread. Note the linear relation.

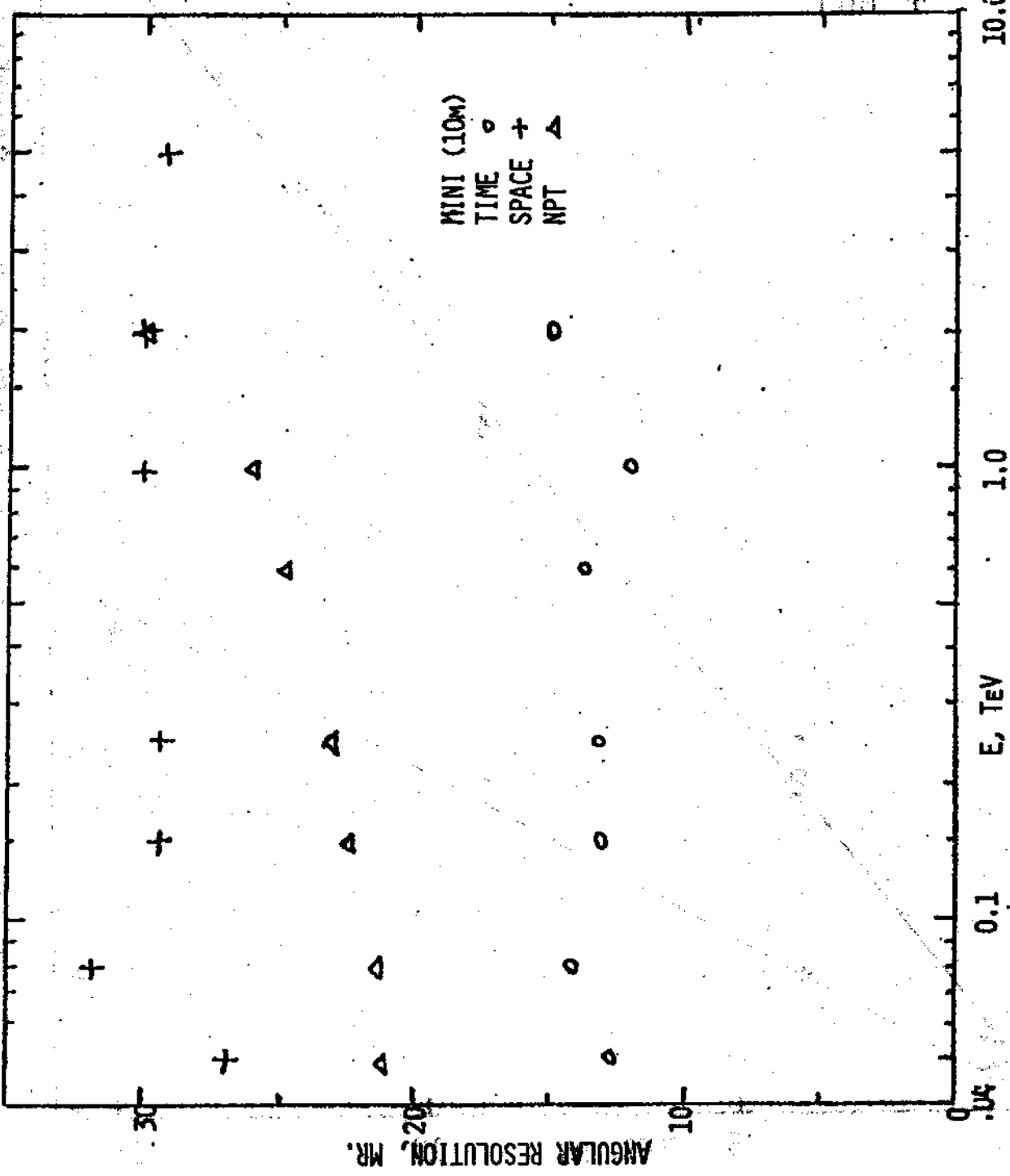


Fig. 2. NPT, the number of hits above a threshold (in this case 3 photoelectrons) and also time and space hits, as a function of muon energy in the MINI array. For Figs. 2 - 6 the water transparency is 25%, the time resolution TRES = 4 ns. The sensor sensitivity is  $S = 1$ .

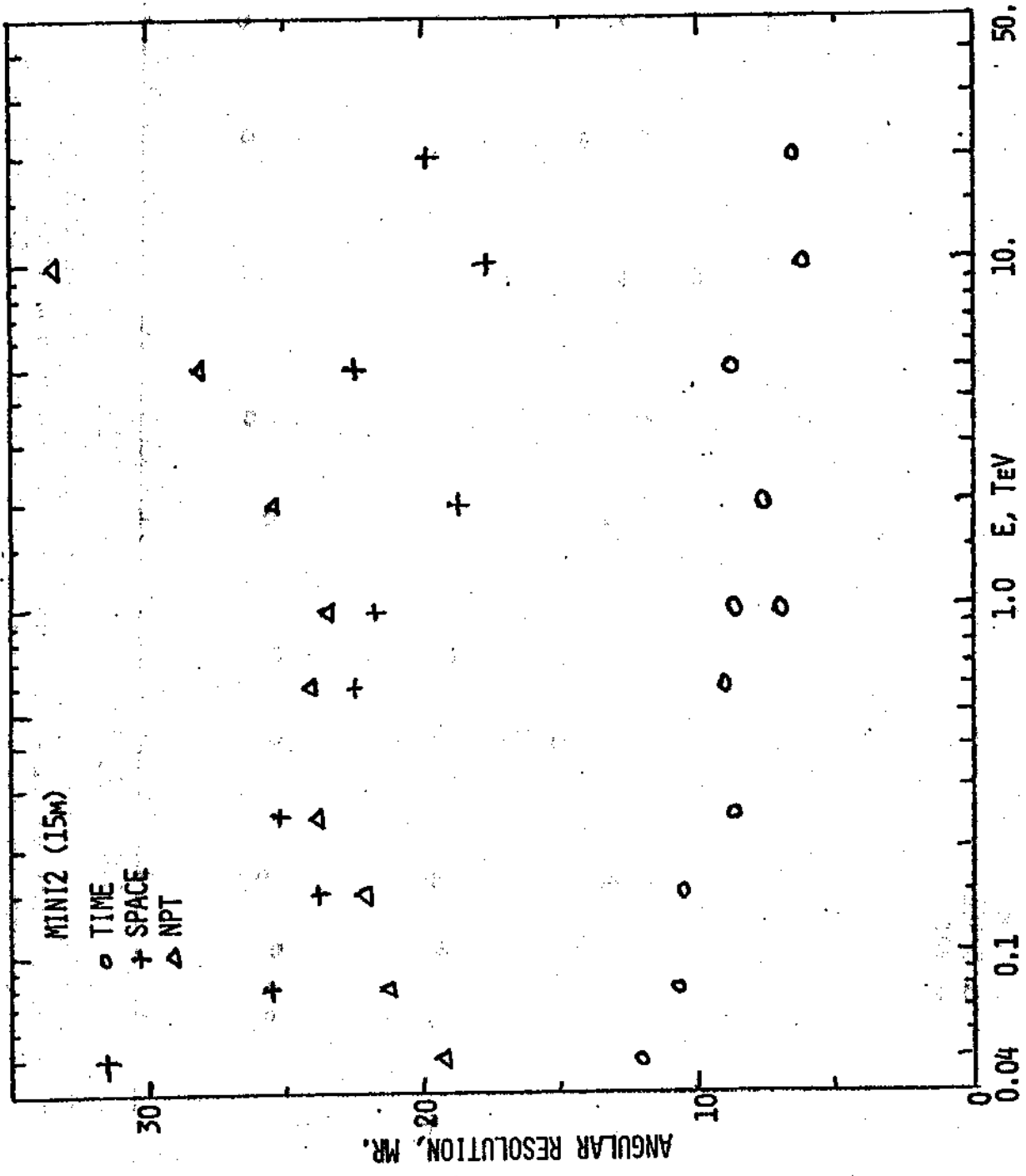


Fig. 3. NPT, time and space fits in MINI2. The sensor threshold is now 2 photoelectrons, as it is for all arrays of 15m spacing or above. The improved resolution is due to the larger size. Sensor sensitivity is  $S = 1$ .

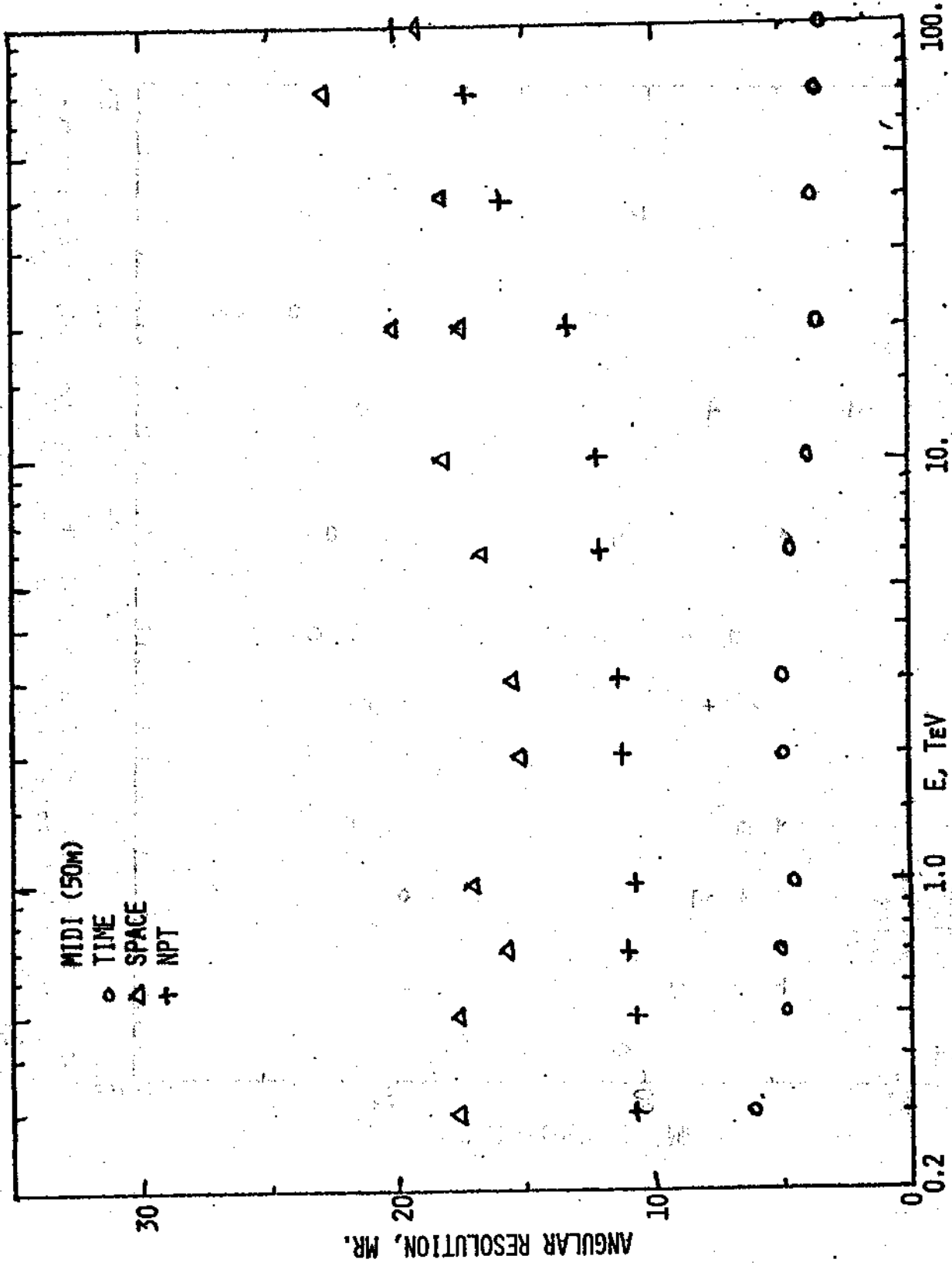


Fig. 4. The same data for MIDI, with 50m spacing. The sensor sensitivity is now  $S = 6$ . At the lower energies, the curve ends when the muon no longer has enough range to traverse the array. Note the excellent resolution from 0.3 to 100 TeV.

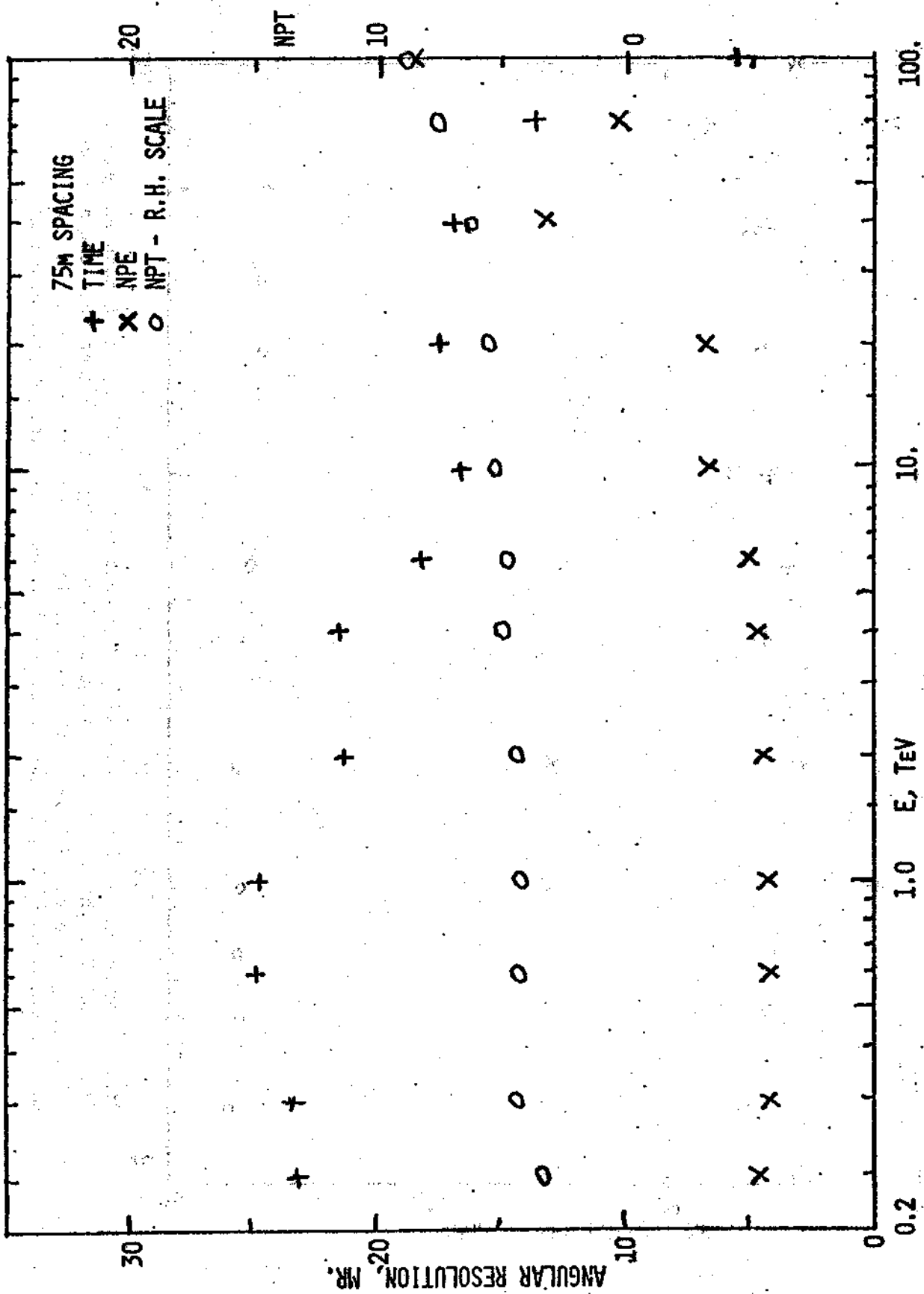


Fig. 5. Performance of an array with 75m spacing,  $S = 6$ . The track allows a good fit only for energies above 50 TeV.

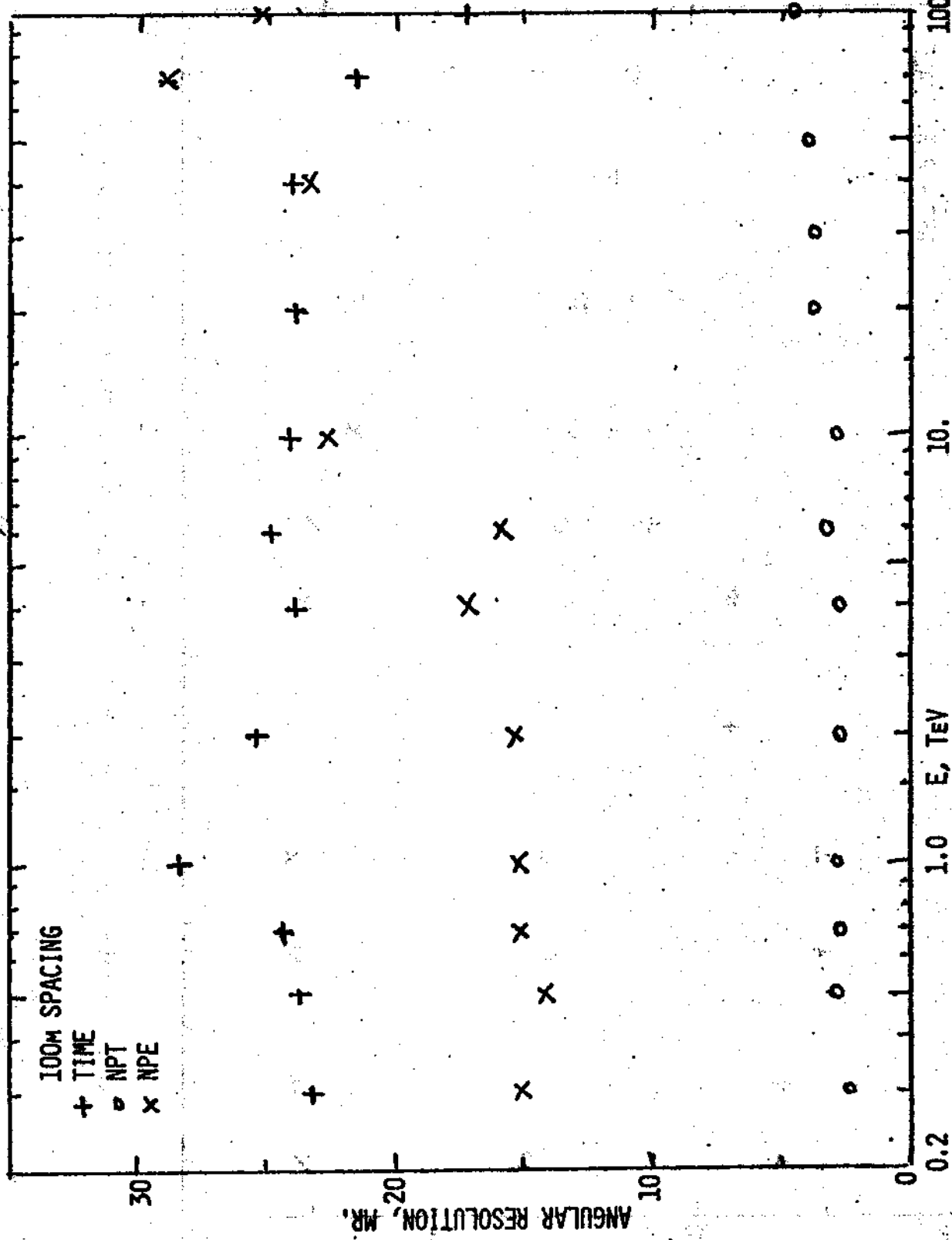


Fig. 6. Performance of an array with 100m spacing, as a function of muon energy.

Even at 100 TeV the performance is poor. The spacing is so great that the average number of photoelectrons per hit, NPE, is 15 or more; this implies that the muon track itself is no longer detected, but only the large bursts along it.

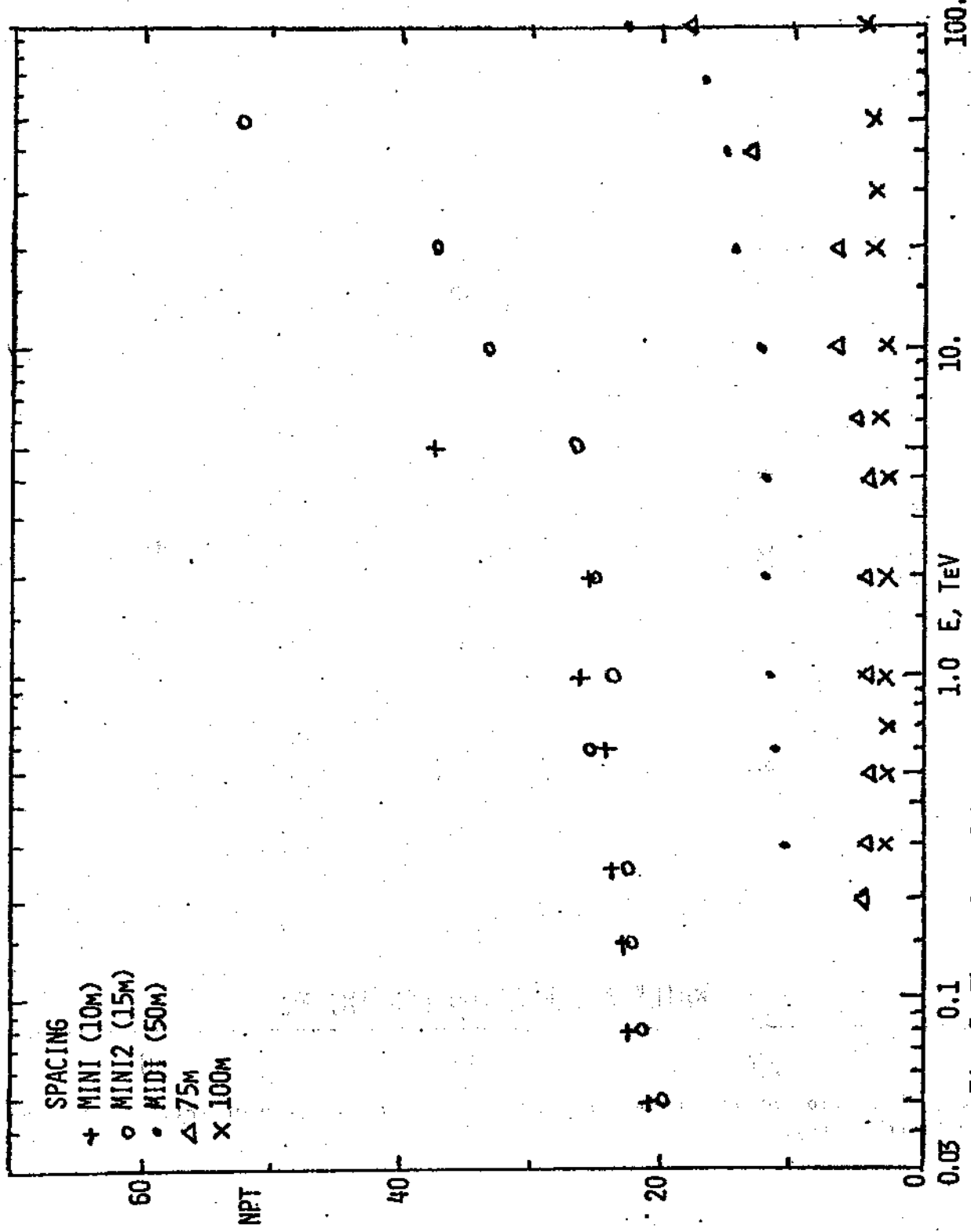


FIG. 7. The number of hits on a track, NPT, for five different spacings, as a function of muon energy. Note that each array has the same number of sensors. Note the tendency to increase at high muon energies.

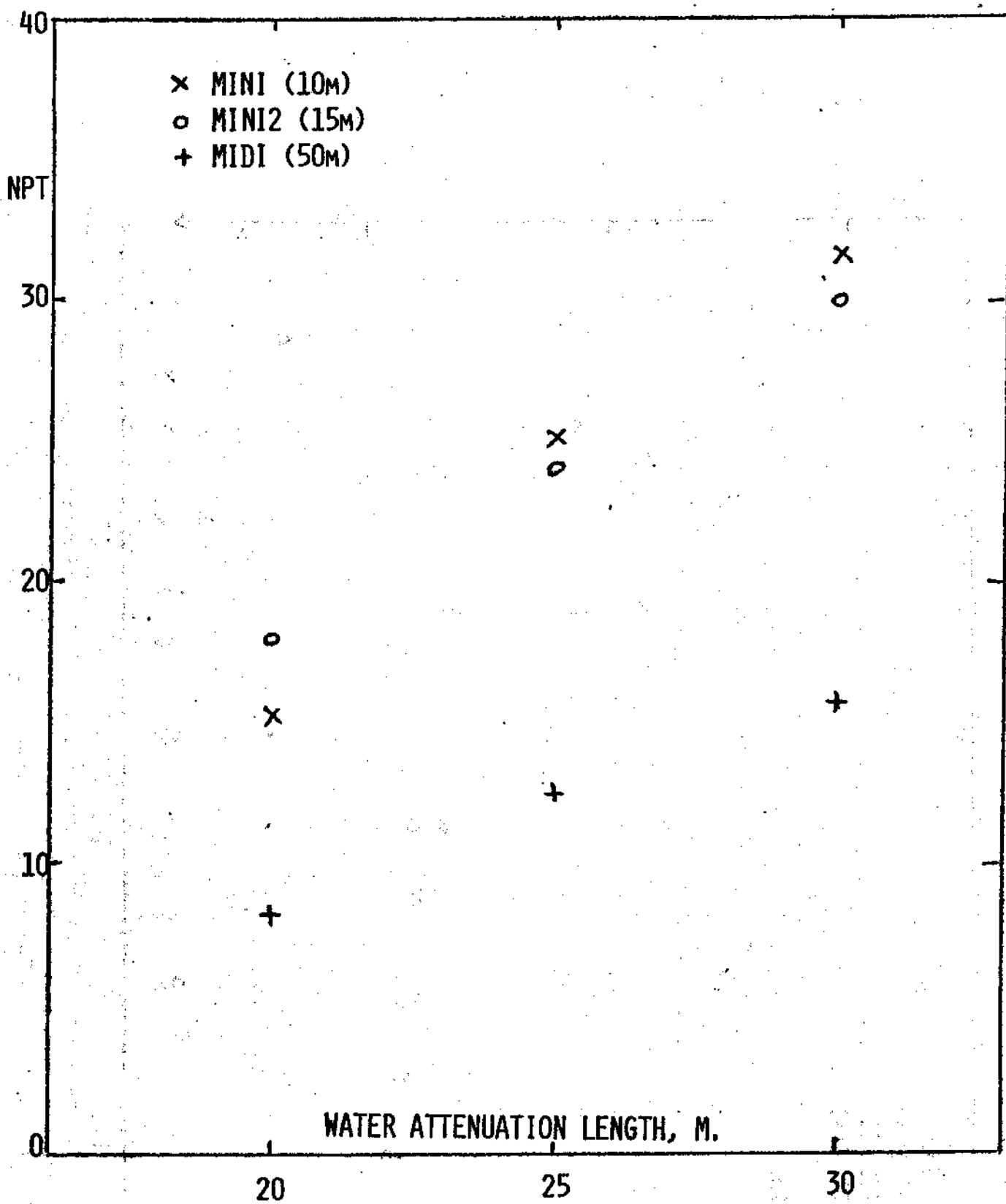


Fig. 8. Variation of the number of hits, NPT, as a function of water transparency, at a fixed energy.

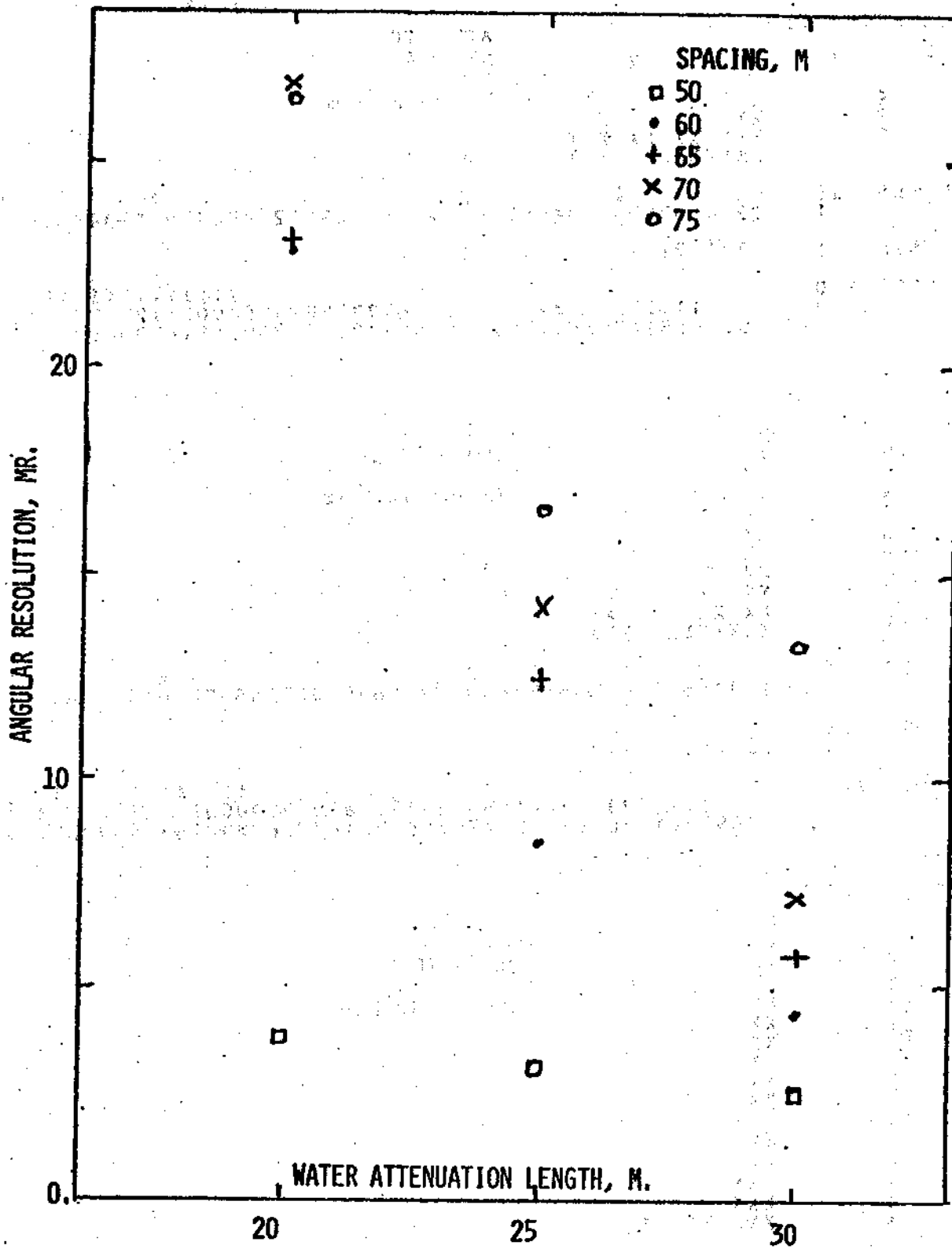


Fig. 9. Angular resolution vs. water transparency for a number of different spacings. The energy is fixed (4 TeV). Note that at 50m spacing, the signals are strong enough at all transparencies to get good resolution; at higher spacings, the deterioration with lower transparency is apparent.

## ANG. ERROR TIME FIT

HBOOK

ID = 433122122

2

ATT = 20m

NPT = 4.75

4

X  
XXX  
XXX XX XX XXX  
XXXXXX XXXX XXXX X X X

Mean = 23.3 mr

CHANNELS

10

0 1 2 3 4 5 6 7 8 9 0 1 2 3 4 5 6 7 8 9 0 1 2 3 4 5 6 7 8 9 0 1 2 3 4 5 6 7 8 9 0 5

CONTENTS

10

-1. 433122122 2431 1 1 1

LOW-EDGE 100

10

111222333344455566667778889990001112222333444  
1. 3692581470369258147036925814703692581470369258147

HBOOK

ID =

2

11

X  
X  
XX  
XXXXXX XXXX XXXX X X X

ATT = 25m

NPT = 7.53

Mean = 12.5 mr

CHANNELS

10

0 1 2 3 4 5 6 7 8 9 0 1 2 3 4 5 6 7 8 9 0 1 2 3 4 5 6 7 8 9 0 5

CONTENTS

10

1. 1912412 132 1

LOW-EDGE 100

10

111222333344455566667778889990001112222333444  
1. 3692581470369258147036925814703692581470369258147

HBOOK

ID =

2

16

X  
X  
XX  
XXX  
XXX  
XXX XX X X

ATT = 30m

NPT = 10.1

Mean = 5.71 mr

CHANNELS

10

0 1 2 3 4 5 6 7 8 9 0 1 2 3 4 5 6 7 8 9 0 1 2 3 4 5 6 7 8 9 0 5

CONTENTS

10

1. 633 11 1 1

LOW-EDGE 100

10

111222333344455566667778889990001112222333444  
1. 3692581470369258147036925814703692581470369258147

Fig. 10. Histograms of time fit for the 65m spacing in Fig. 9.

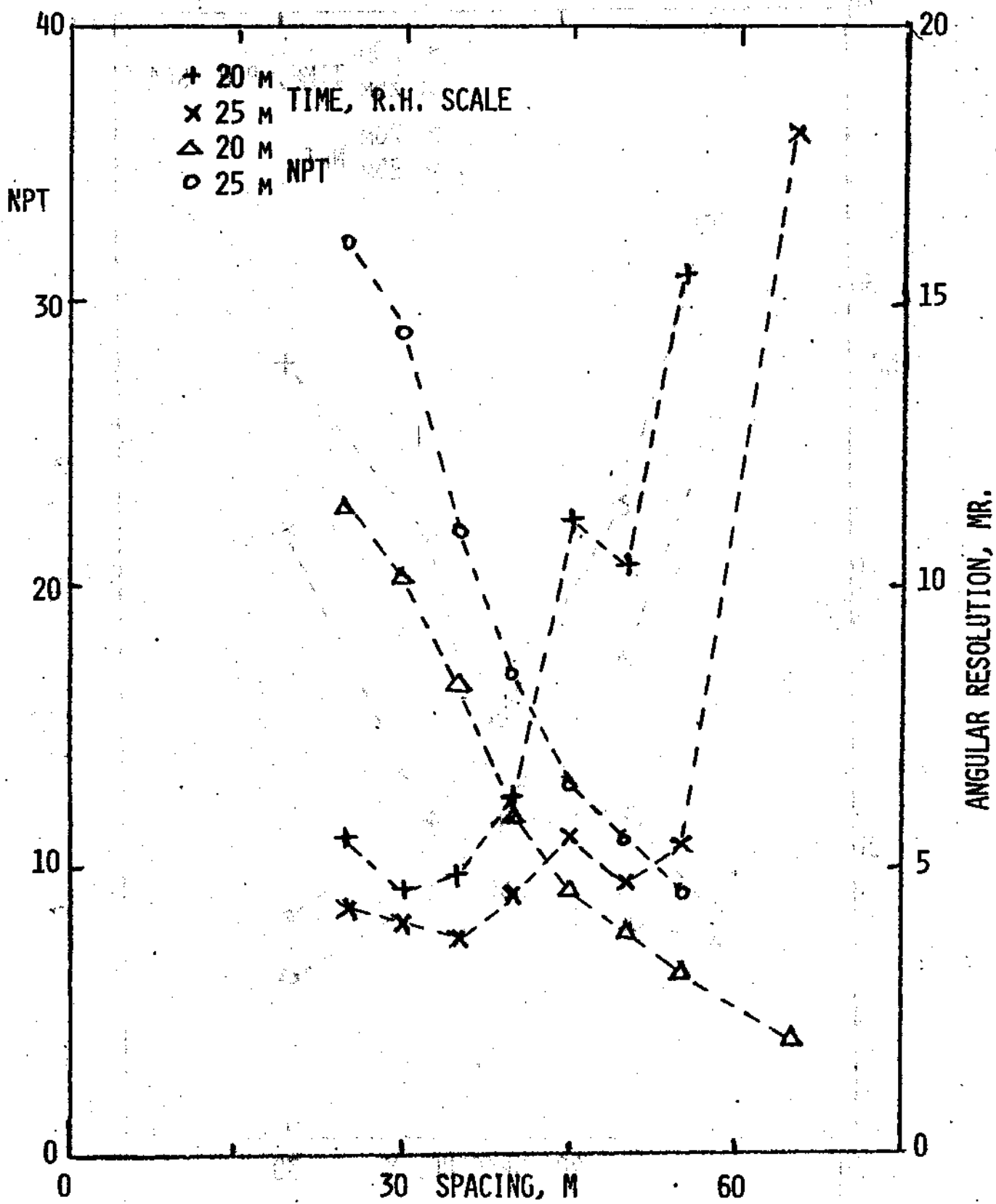


Fig. 11. Variation of the number of hits and the time fit with array spacing, for two different water transparencies. Sensor sensitivity is constant at  $S = 6$ , muon energy at 1 TeV. The dotted lines are added to guide the eye. Note, e.g., that for 25m transparency, the time fit remains good until the spacing exceeds 55m; this defines the "knee" of the resolution curve.

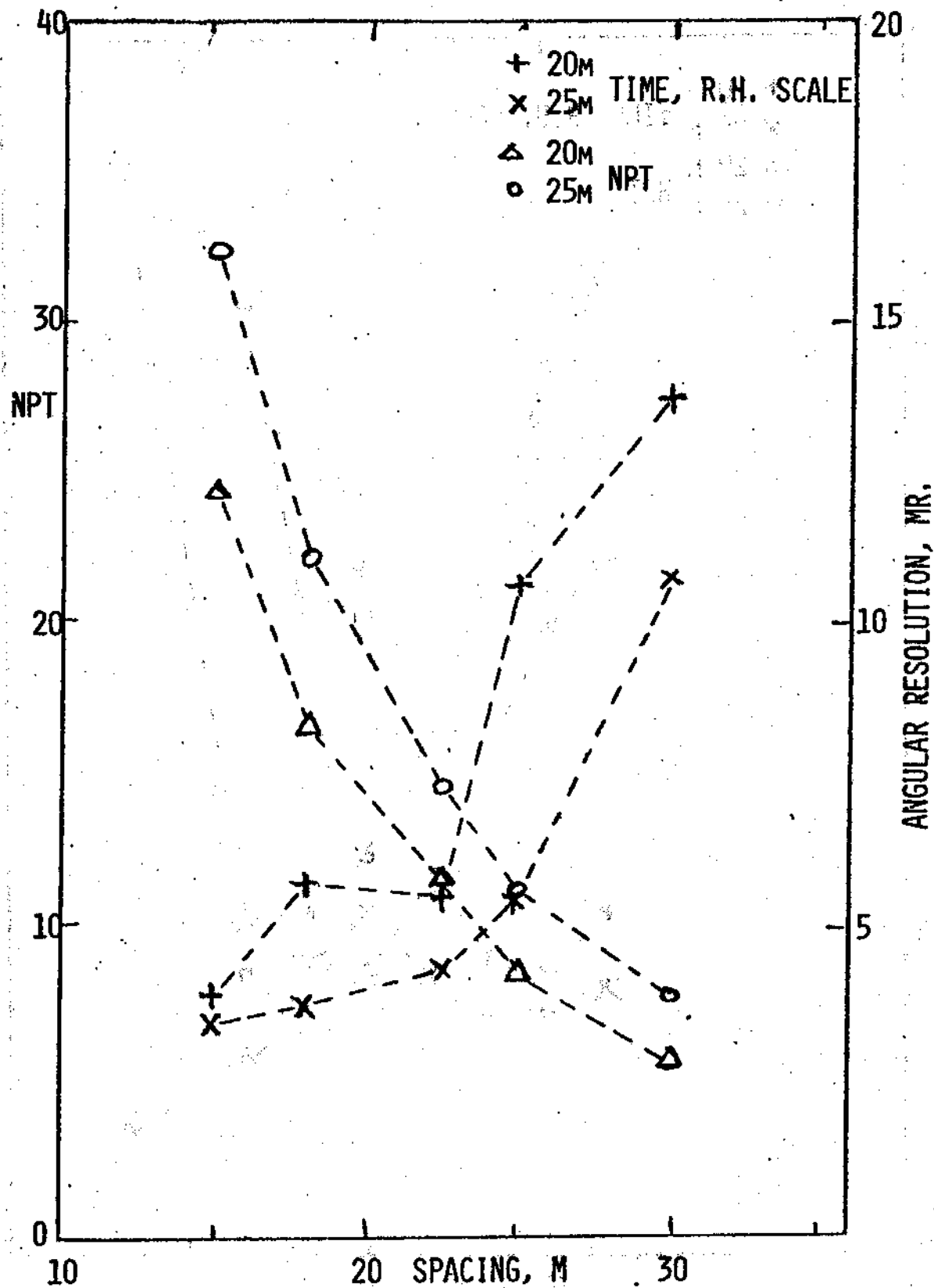


Fig. 12. The same as Fig. 11, except that the sensor sensitivity is  $S = 1$ . The "knee" for 25m water is at a spacing of 25 meters.

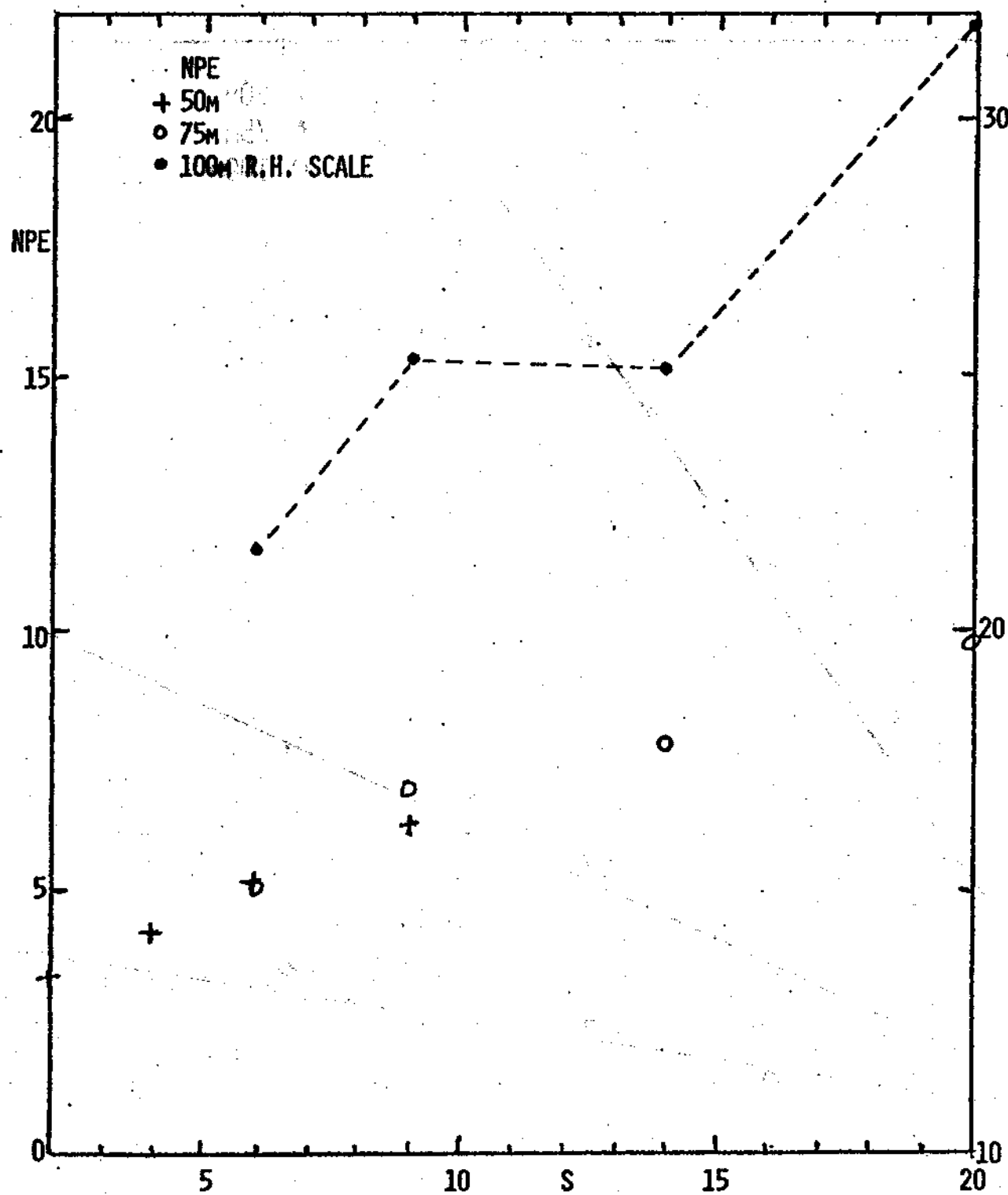


Fig. 13. The average number of photoelectrons per hit, NPE, as a function of S for large array spacings. The threshold is 2 photoelectrons. The 100m array, with the largest number, has the fewest hits and the poorest fits. It sees only large bursts on distant tracks.

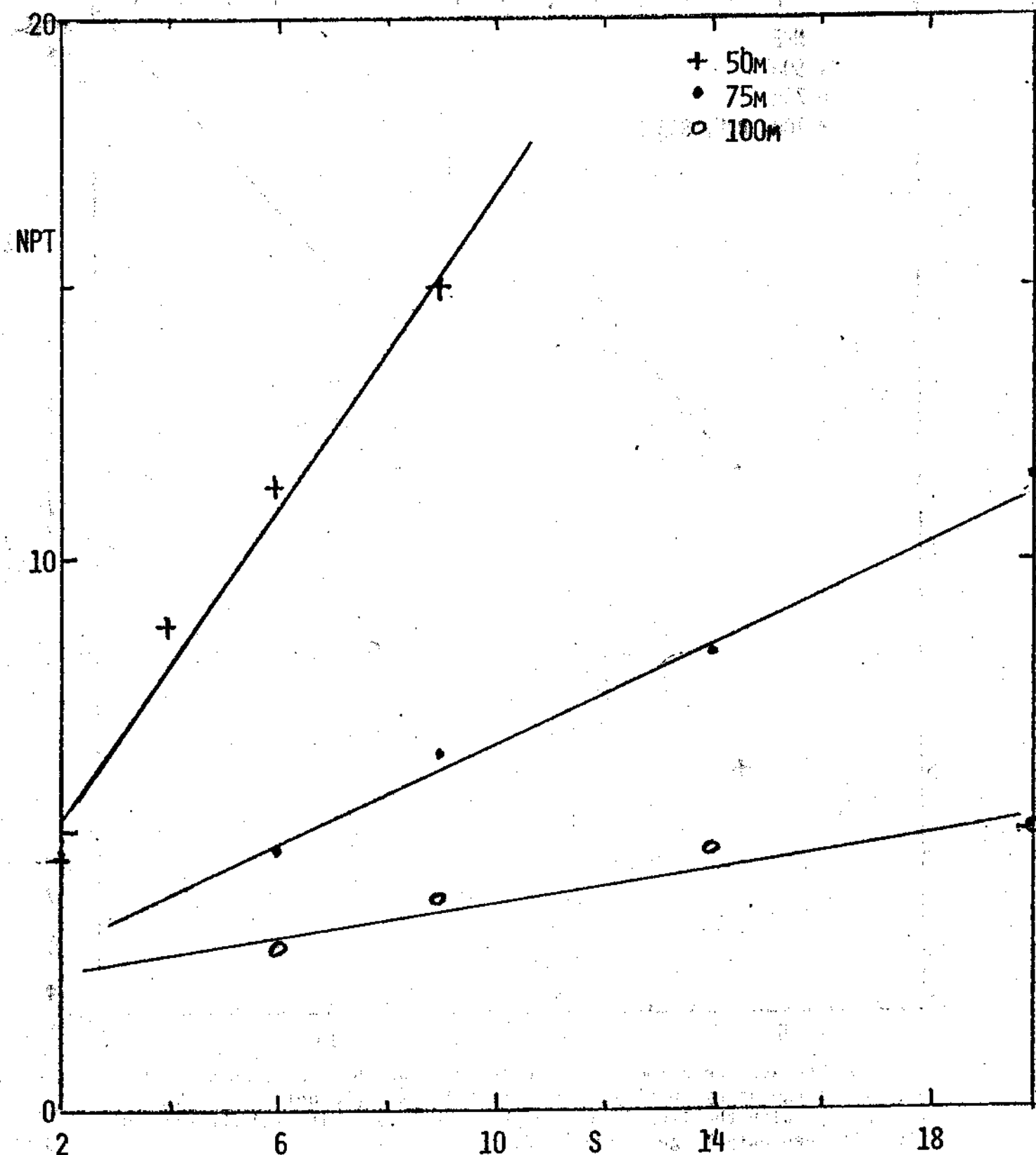


Fig. 14. The relation between the number of hits,  $NPT$ , and the detector sensitivity  $S$ , as a function of array spacing. The increase is less rapid than  $S$ ; hence the slow improvement of array performance with increasing  $S$ .

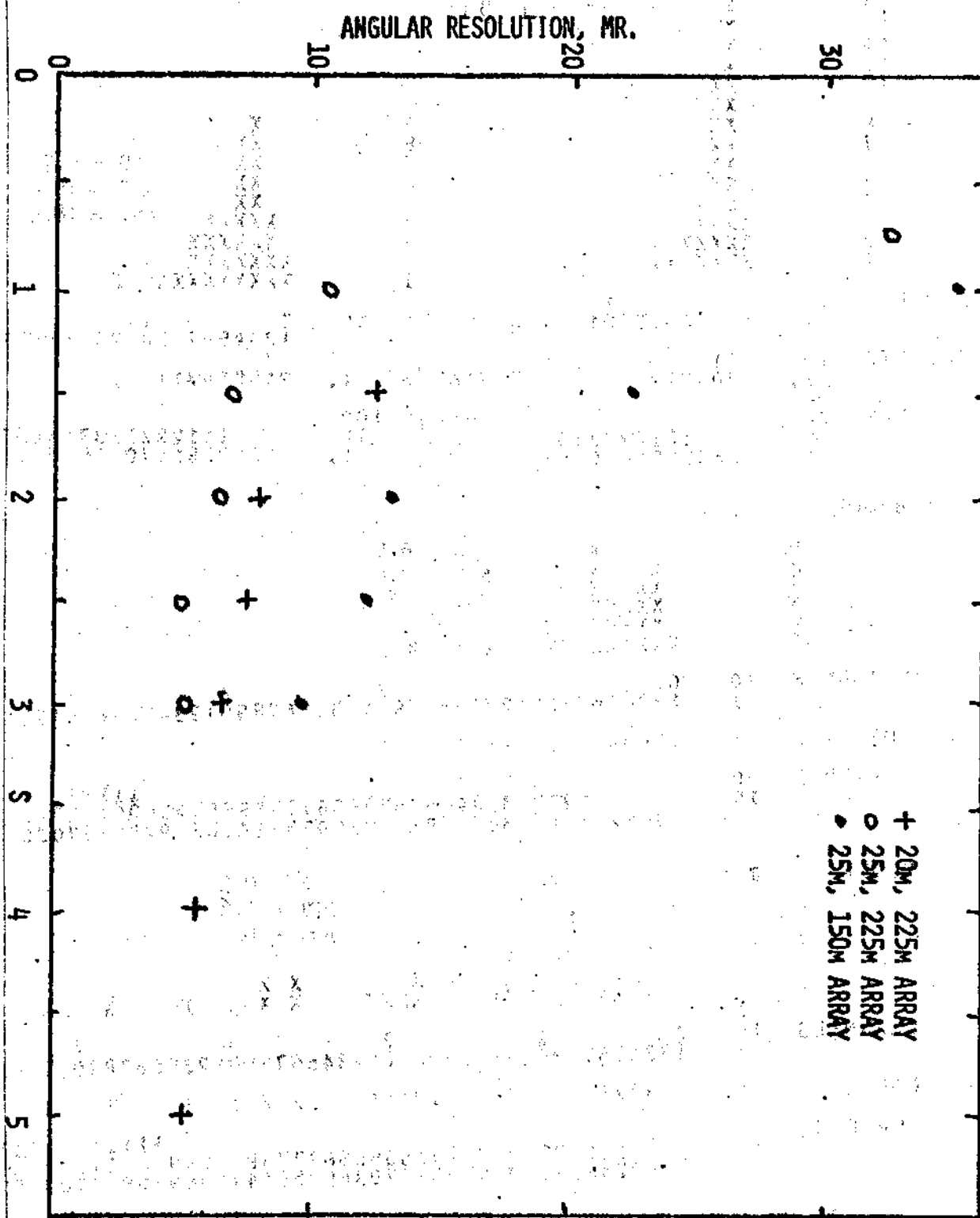


Fig. 15. Curves for 22.5m array spacing, showing time fit vs. detector sensitivity for two values of the water transparency; and also for a smaller array, 150m long instead of 225m, which requires higher sensitivity and yields poorer performance.

## ANG. ERROR TIME FIT

24

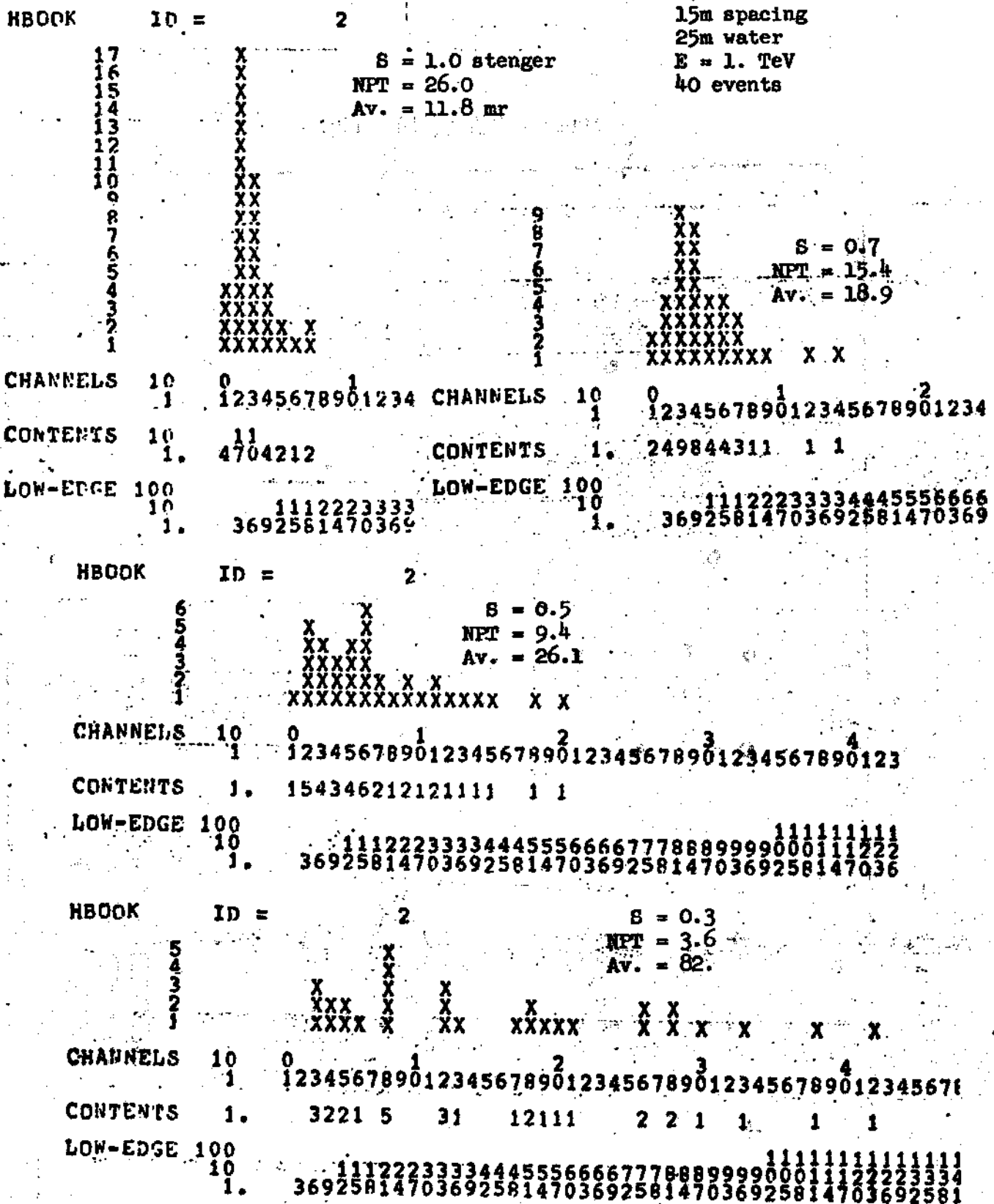


Fig. 16. Histogram of time fits for 15m array, as detector sensitivity S is varied. Energy 1 TeV, transparency 25m.

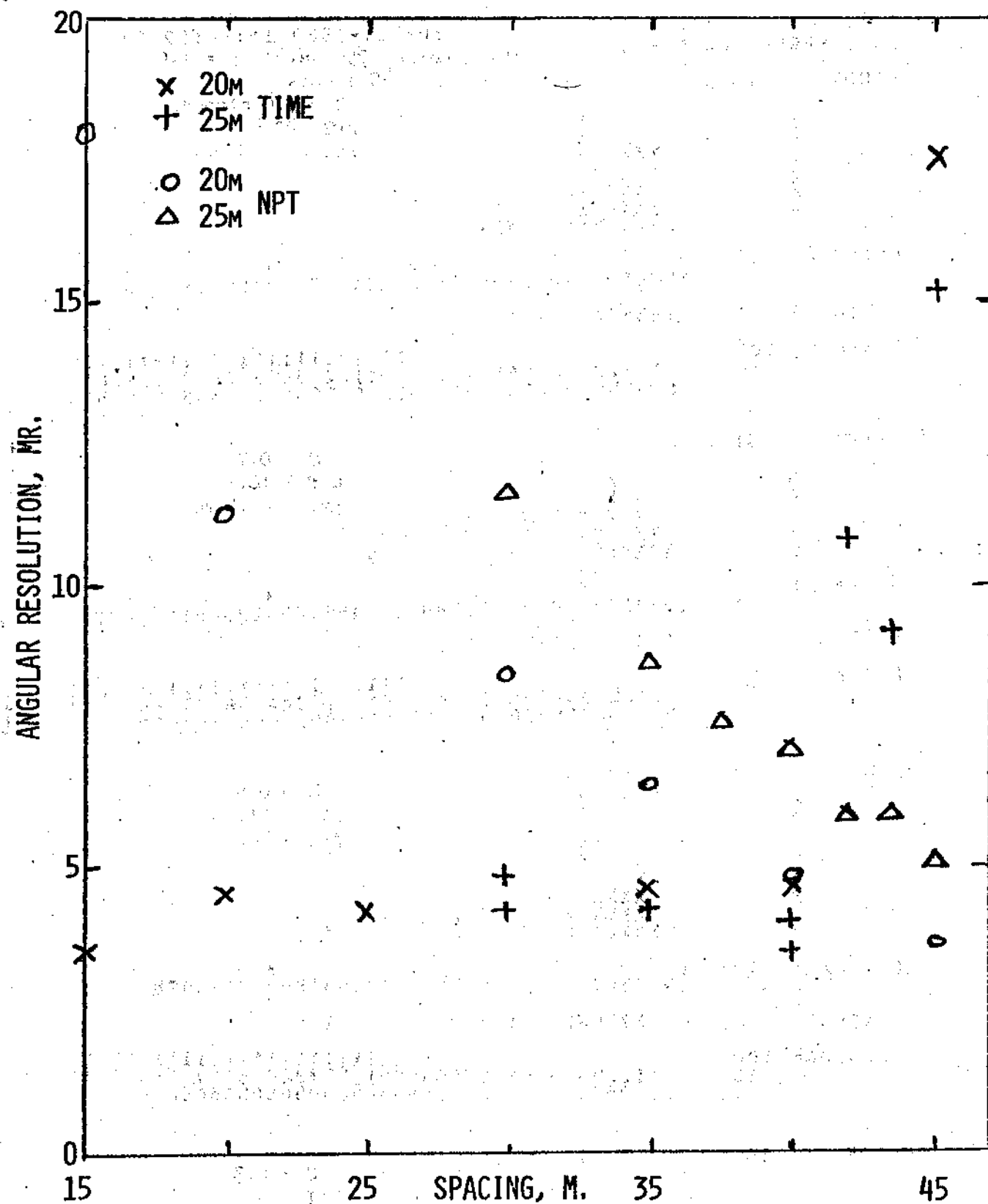


Fig. 18. Properties of double-length arrays: each cubic array is twice as large, with 21 detectors on each edge. Thus 25m spacing refers to an array 500m on a side. The effects are a) large improvement in angular resolution, b) much larger spacings permissible for the same detector sensitivity. These data are for  $S = 1$ , which we note now allows 40m spacing. Compare Fig. 12, which shows similar data for single-length arrays.

## ANG. ERROR SPACE FIT

30-OCT-1980 11:44:52.53

15m spacing, 25m water, E = 1.0 TeV

HBOOK ID = 1

40 events

S = 2.0 stenger

NPT = 2334

Av. = 31.7 mr.

7		X	X
6		X	X
5		XXX	X
4		XXX	XX
3		XXXXXX	
2		XXXXXX	X
1		XXXXXXXXX	XXX

 CHANNELS 10 0 1 2 3 4  
 1 12345678901234567890123456789012345678901234

CONTENTS 1. 1655347311 121

 LOW-EDGE 100 100 1111111111111111111112222  
 10 112233445566778899001122334455667788990011  
 1. 505

HBOOK ID = 1

S = 0.7

NPT = 16.2

Av. = 44.2 mr

5		X	
4		XX	X
3		XXXXX	XX
2		XXXXX	XX
1		XXXXXXXX	XX XX X X

 CHANNELS 10 0 1 2 3 4  
 1 12345678901234567890123456789012345678901234

CONTENTS 1. 124154334 33 23 1 1

 LOW-EDGE 100 100 1111111111111111111112222  
 10 112233445566778899001122334455667788990011  
 1. 505

HBOOK ID = 1

S = 0.5

NPT = 11.5

Av. = 46.1

8		X	
7		X	
6		XX	
5		XX	
4		XX	
3		XXXX	
2		XXXXX	X X X
1		XXXXXX	XXXX X X X X X

 CHANNELS 10 0 1 2 3 4  
 1 12345678901234567890123456789012345678901234

CONTENTS 1. 1533682 21112 2 1 1 1

 LOW-EDGE 100 100 1111111111111111111112222  
 10 112233445566778899001122334455667788990011  
 1. 505

HBOOK ID = 1

S = 0.3

NPT = 5.9

Av. = 99.

5		X	
4		X	
3		X	XXX
2		XX	XXX X
1		XXX	XXXXXXX X X X X X XXX

 CHANNELS 10 0 1 2 3 4  
 1 12345678901234567890123456789012345678901234

Fig. 17. Same as Fig. 16, for space fit (no timing information)

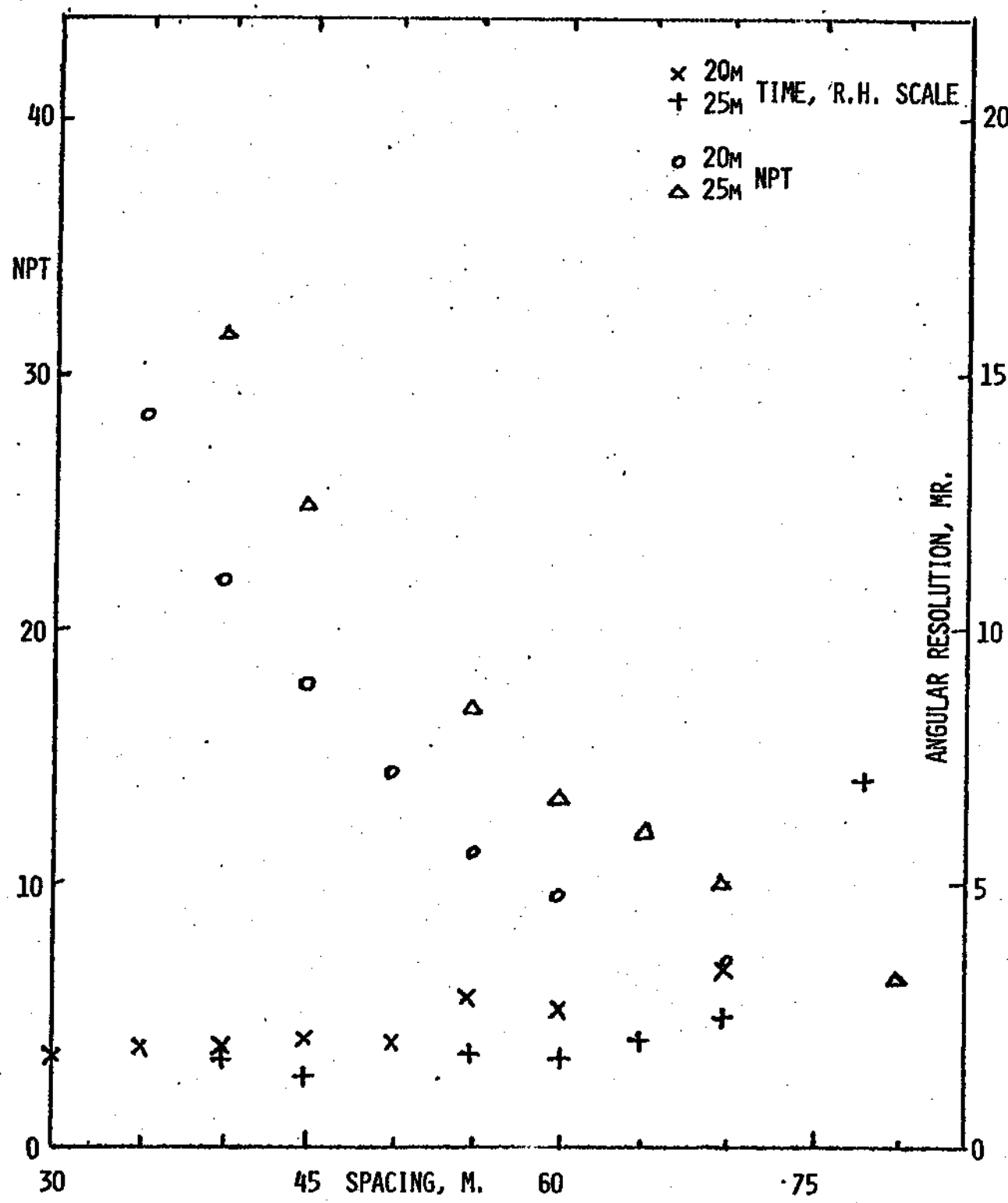


Fig. 19. Double-length array properties for  $S = 6$ . Note that spacings up to 70m are possible. Angular resolutions better than 2 mr are achieved. Compare Fig. 11 for single-length arrays.

